RSC Advances

PAPER

View Article Online
View Journal | View Issue

Open Access Article. Published on 24 November 2025. Downloaded on 1/19/2026 3:43:59 PM.
This article is licensed under a Creative Commons Attribution-NonCommercial 3.0 Unported Licence.

Check for updates

Cite this: *RSC Adv.*, 2025, **15**, 46207

Green "turn-off" luminescent nanosensor for the sensitive analysis of finerenone in various matrices: application of recent greenness assessment techniques

Mohamed B. Ali,[a] Ahmed M. Abdel-Raoof,*[b] Hadil M. Elbardisy,[a] Gamal A. Omran,[c] Mahmoud A. Ragab[d] and Samir Morshedy[a]

Finerenone (FNR) is an innovative FDA-approved selective non-steroidal mineralocorticoid receptor antagonist utilized in kidney failure. This study utilizes eco-friendly nitrogen and sulfur co-doped carbon quantum dots (N,S-CQDs), fluorescent nanomaterials, to introduce a sensitive and environmentally sustainable spectrofluorometric platform for the analysis of FNR. Water-soluble N,S-CQDs were prepared from green precursors (citric acid and glutathione) using a straightforward and eco-friendly hydrothermal technique. The intrinsic fluorescence of the fluorophore was monitored at $\lambda_{em} = 419$ nm upon excitation at 344 nm. The luminescence of the fluorophore was quantifiably dropped after the incorporation of FNR, which is the foundation of this luminescent technique. The luminescence quenching mechanism was investigated, and the suggested methodology was validated in compliance with the ICH considerations. The analytical response for FNR was achieved throughout the linear dynamic range of 0.30 to 9.00 μg mL^{-1}. The calculated limits for FNR detection and quantification were 0.098 and 0.297 μg mL^{-1}, respectively. The suggested approach was utilized for the analysis of FNR in authentic powder, commercial formulation, and spiked human plasma. The computed percentage recoveries and percentage relative standard deviations were acceptable. The assessment of the ecological sustainability of the suggested approach, utilizing recently developed methodologies, including the Blue Applicability Grade Index (BAGI), the Complex Modified Green Analytical Procedure Index (ComplexMoGAPI), and the Carbon Footprint Reduction Index (CaFRI), has shown its superiority and sustainability compared to the reported methodologies for the FNR analysis.

Received 14th October 2025
Accepted 18th November 2025

DOI: 10.1039/d5ra07857a

rsc.li/rsc-advances

1. Introduction

Finerenone (FNR), also known as BAY 94-8862, is a new selective non-steroidal mineralocorticoid receptor antagonist (MRA) characterized by the chemical structure (4S)-4-(4-cyano-2-m-ethoxyphenyl)-5-ethoxy-2,8-dimethyl-1,4-dihydro-1,6-naphthyridine-3-carboxamide[1,2] (Fig. 1A). It is recommended to mitigate cardiovascular and renal issues in people with chronic kidney disorder related to type II diabetes mellitus.[2] FNR functions by obstructing the impact of mineralocorticoids, including cortisol and aldosterone, at the mineralocorticoid receptor, thereby preventing its activation and diminishing inflammation in the heart and kidneys.[2] In contrast to previous steroidal MRAs like spironolactone, FNR provides the advantage of not inducing androgenic adverse effects such as gynecomastia or sexual dysfunction due to its superior selectivity for MR receptors over androgen receptors.[2,3] Moreover, because of the short half-life of FNR and the absence of active metabolites, it could lead to a diminished risk of hyperkalemia in comparison to spironolactone.[2,3] FNR is marketed under the brand name Kerendi and is available in the pharmaceutical market as 10 mg and 20 mg film-coated tablets.[4]

In July 2021, FNR received approval for medicinal application from the U.S. Food and Drug Administration (FDA),[5] and in February 2022, it was authorized by the European Medicines Agency (EMA) in the European Union.[6]

After a comprehensive examination of the FNR reported methods, it was determined that only a limited number of studies have been published about its precise analysis. The approaches encompass the following: spectrophotometry,[7,8] fluorometry,[9] and high-performance liquid chromatography.[10–12]

[a]Pharmaceutical Analytical Chemistry Department, Faculty of Pharmacy, Damanhour University, Damanhour, Egypt. E-mail: Mohamed.ali@pharm.dmu.edu.eg
[b]Pharmaceutical Analytical Chemistry Department, Faculty of Pharmacy, Al-Azhar University, Cairo, Egypt
[c]Department of Biochemistry, Faculty of Pharmacy, Damanhour University, Damanhour, Egypt
[d]Pharmaceutical Chemistry Department, Faculty of Pharmacy, Damanhour University, Damanhour, Egypt

© 2025 The Author(s). Published by the Royal Society of Chemistry

Open Access Article. Published on 24 November 2025. Downloaded on 1/19/2026 3:43:59 PM.
This article is licensed under a Creative Commons Attribution-NonCommercial 3.0 Unported Licence.

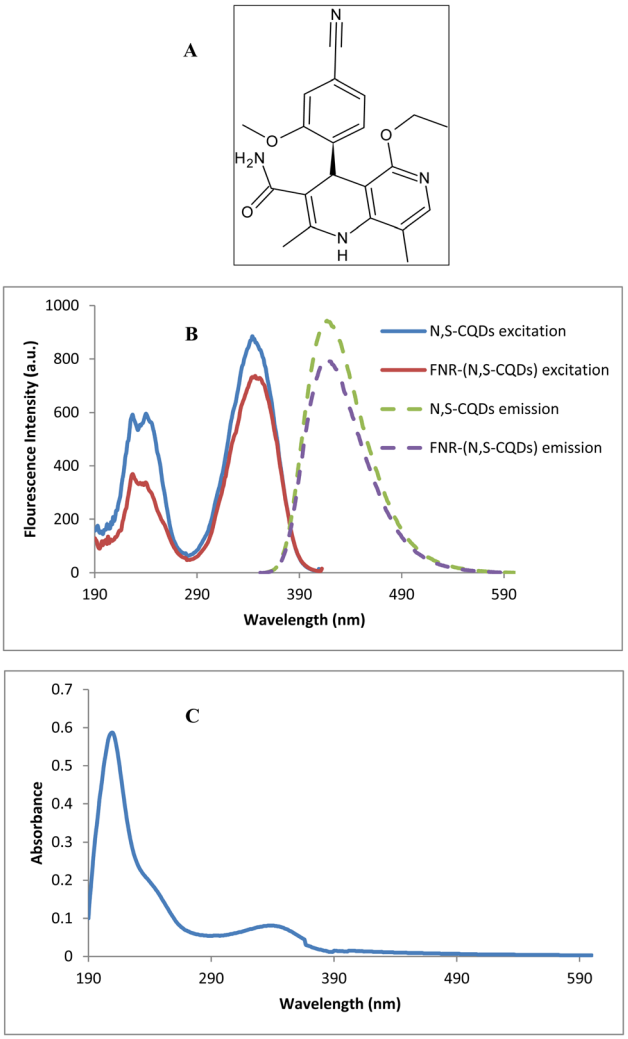

Fig. 1 (A) Chemical structures of finerenone (FNR), (B) excitation and emission spectra of N,S-CQDs in the presence and absence of 3 μg mL^{-1} of FNR (λ excitation = 344 nm, λ emission = 419 nm, with excitation/emission slit widths of 5 nm), and (C) UV-visible absorption spectrum of N,S-CQDs.

Carbon quantum dots (CQDs) are specialized fluorescent nanosensors and possess exceptional electric and optical characteristics, coupled with their diminutive dimension and high surface area, rendering them highly advantageous for analytical and technological purposes.[13] CQDs are widely utilized as alternate fluorescent nanomaterials for analytical studies instead of using semiconductor quantum dots or fluorescent dyes, as a result of their minimal toxic behaviors, high water solubility, adjustable emission wavelengths, and superior photostability.[14,15] Numerous strategies have been established for the production of fluorescent CQDs, such as microwave-assisted methods,[16] hydrothermal cutting techniques,[17] chemical and electrochemical oxidation,[18–21] and carbonization.[22,23] The aforementioned approaches generally generate low yields and require costly equipment, making them undesirable. N and S co-doped carbon quantum dots (N,S-CQDs) are extensively utilized in various studies, as the reactive areas of the CQDs are enhanced by the fact that N possesses 5 valence electrons available for reacting with C atoms in the CQDs.[13] The electrical configuration of CQDs can be altered by S atoms, which prevent self-quenching as a result of their significant Stokes shift.[13] The co-doping of N and S demonstrated exceptional luminescence characteristics, substantial chemical stability, little toxicity, heightened sensitivity, and elevated quantum yield.[13]

Inspired by the above insights, this study employed a simple hydrothermal method to synthesize N,S-CQDs from citric acid and glutathione. Citric acid functioned as the carbon supply, whilst glutathione functioned as the source of sulfur and nitrogen. This method provides a straightforward, sensitive, and fast analysis of FNR in raw material, commercial formulation, and human plasma. The estimation of FNR relied on the quenching of the fluorophore *via* the inner filter effect. Additionally, a prominent focus of contemporary research pertains to the application of eco-friendly methodologies. For this purpose, recent greenness assessment tools, including the complex modified green analytical procedure index (Complex-MoGAPI),[24] the blue applicability grade index (BAGI),[25] and the carbon footprint reduction index (CaFRI),[26] were applied in this work. Finally, the developed approach serves as a method of analysis suitable for detecting and quantifying FNR in quality control laboratories.

2. Experimental

The SI section contains a complete description of the instruments and chemicals employed in this work.

2.1. Stock and working FNR solutions

100 μg mL^{-1} of standard FNR solution was produced by adding 0.01 g of FNR to 100 mL of methanol. For one week, the FNR stock solution was kept in the refrigerator at 4 °C. The stock solution was diluted with deionized water to get the specified final concentrations in order to produce working solutions.

2.2. Preparation of N,S-CQDs

Initially, 10 mL of deionized water was used to dissolve anhydrous citric acid (1.82 g, 9.5 mmol) and reduced glutathione (2.56 g, 8.34 mmol). The solution was treated *via* ultrasonic dispersion for 5 minutes to reach complete dissolution. The mixture was then subjected to heating in a convection oven at 70 °C for 12 hours, yielding a thick mixture. Using a 30 mL Teflon-lined stainless-steel autoclave reactor, the syrup was heated at 200 °C for 3 hours at a heating rate of 10 °C min^{-1}. The product obtained from the reaction was subjected to cooling at room temperature. After that, the produced black product was diluted with deionized water to reach a final volume (100 mL) and sonicated for 5 min. A membrane filter (0.22 μm) was used to filter the suspension to remove larger aggregates, and the filtrate was neutralized to pH 7 by adding sodium bicarbonate. For purification, a dialysis membrane (MWCO = 1000 Da) was used for 48 h; the water was changed every 6 h to remove unreacted precursors and other impurities. The purified product suspension was collected for further analysis. For solid-

 © 2025 The Author(s). Published by the Royal Society of Chemistry

Open Access Article. Published on 24 November 2025. Downloaded on 1/19/2026 3:43:59 PM.
This article is licensed under a Creative Commons Attribution-NonCommercial 3.0 Unported Licence.

state characterizations such as FTIR and TEM, an aliquot of the purified solution was subjected to freeze-drying to get a solid powder substance.

2.3. Experimental procedures

To establish a calibration curve for FNR, accurate amounts from the FNR stock solution, to obtain the final concentration range of 0.30–9.00 μg mL^{-1}, were placed into 10 mL volumetric flasks, to which 10 μL of N,S-CQDs (0.095 M) was transferred to each flask, then 2 mL of Britton–Robinson buffer (BR-buffer) was added. After that, the solution was diluted with deionized water until it reached the mark. The working solutions' luminescence intensities were quantified at λ_{em} of 419 nm, upon excitation at 344 nm. The measurements were subtracted from the related reading of a blank subjected to similar treatment. The calibration curve was developed by graphing the differences in luminescence intensity relative to the relative FNR concentration (μg mL^{-1}).

2.4. Application procedures

2.4.1. Estimation of FNR pharmaceutical dosage form. Ten tablets (Finoxlab®, 20 mg) were meticulously pulverized and homogeneously mixed. A sufficient amount of the resulting powder was added to a 100 mL volumetric flask, and the extraction procedure was conducted with methanol (40.0 mL). The mixture underwent sonication for 20 minutes, after which methanol was used to complete the flask volume, and then the sonication was performed for another 20 minutes. The mixture was filtered, and deionized water was employed for additional dilutions. The analysis procedure was executed as previously described in the experimental procedures section, and then the regression equation was used to estimate the FNR concentration.

2.4.2. Estimation of FNR in spiked human plasma. Plasma specimens containing 0.5 mL were inserted into a series of centrifuge containers. The samples were then filled with various FNR amounts, and the tubes were appropriately vortexed. For protein precipitation, 1 mL of acetonitrile was loaded, and the resultant mixture underwent centrifugation for 20 minutes at 8000 rpm. To determine FNR concentration, 1 mL of the resultant supernatant was extracted and diluted with an adequate volume of deionized water. The FNR was then analyzed following the previously specified steps described in the experimental procedure section.

3. Results and discussion

3.1. Physicochemical characterization of N,S-CQDs

UV-vis spectrophotometry and spectrofluorimetry were utilized to assess the optical properties of the prepared fluorophore. Fig. 1B illustrates the fluorescence spectra of N,S-CQDs at λ_{em} of 419 nm upon excitation at 344 nm. A notable quenching of the fluorophore luminescence was observed upon adding 3 μg mL^{-1} of FNR to the fluorophore solution (Fig. 1B). The UV-vis absorption spectrum of the synthesized fluorophore was measured (Fig. 1C), and it revealed two prominent peaks at 209 and 344 nm.

The structure of the prepared fluorophore was verified utilizing the Fourier transform infrared (FTIR) technique (Fig. 2A). The FTIR spectrum of the prepared fluorophore demonstrated a wide absorption band ranging from 3300 to 2500 cm^{-1}, which indicates the O–H stretching vibration of carboxylic O–H. The N–H stretching vibration was detected at 3430 cm^{-1}.15 C=N or C=O in amide appeared around 1683 cm^{-1}.[27] The signal around 1592 cm^{-1} reflects the C=C stretching vibration in the aromatic rings.[28] C=S stretches were observed at 1111 cm^{-1}.[29] Furthermore, the peak around 707 cm^{-1} was related to C–S stretching vibrations,[30] demonstrating the presence of the S atom. Furthermore, TEM images were obtained to assess the morphological properties and dimensions of the CQDs. The prepared fluorophore exhibits a spherical shape as shown in Fig. 2B. The particle size distribution of N,S-CQDs is demonstrated in Fig. S1, where the histogram shows that the most frequent particle size is approximately 2.8 nm, and the normal (Gaussian) distribution was fitted to the data, giving a mean particle size of approximately 4.4 nm.

3.2. Quantum yield

By conducting a comparison with a standard quinine sulfate solution in 0.1 M sulfuric acid, the quantum yield of the synthesized fluorophore was assessed.[31] Multiple diluted concentrations of standard quinine sulfate and fluorophore solutions were made, and their absorbances and fluorescence intensities were measured. The subsequent formula was employed to calculate the quantum yield (Φ) of the fluorophore:

$$\Phi_x = \Phi_{QS}\left(\frac{G_x}{G_{QS}}\right)\left(\frac{\eta_x}{\eta_{QS}}\right)^2$$

The signs (x) and (QS) denote N,S-CQDs, and standard quinine sulfate, respectively. G represents the slopes obtained from the integrated fluorescence *versus* absorbance plots (G_X and G_{QS} were found to be 7.57×10^5 and 7.72×10^5, respectively), and η signifies the refractive index of the solvent. The prepared fluorophore and quinine sulfate were both greatly diluted in deionized water, resulting in similar refractive indices. Knowing that $\Phi_{QS} = 54\%$,[32] Φ_x was determined to be 52.93%.

3.3. Explanation of the quenching mechanism

Different mechanisms can induce fluorescence quenching, including the inner filter effect (IFE), static quenching, and dynamic quenching.[33] Dynamic and static quenching occur due to molecular interactions between the fluorophore and the quencher. Regarding static quenching, a non-fluorescent complex is produced between the fluorophore and quencher. In dynamic quenching, the quencher should diffuse to the fluorophore in the excited state, and the molecules do not undergo permanent alteration due to the quenching. Quenching may occur due to loss of emission groups, energy/electron transfer, collisional quenching, molecular rearrangements, ground-state complex creation, and during excited-state

Open Access Article. Published on 24 November 2025. Downloaded on 1/19/2026 3:43:59 PM.
This article is licensed under a Creative Commons Attribution-NonCommercial 3.0 Unported Licence.

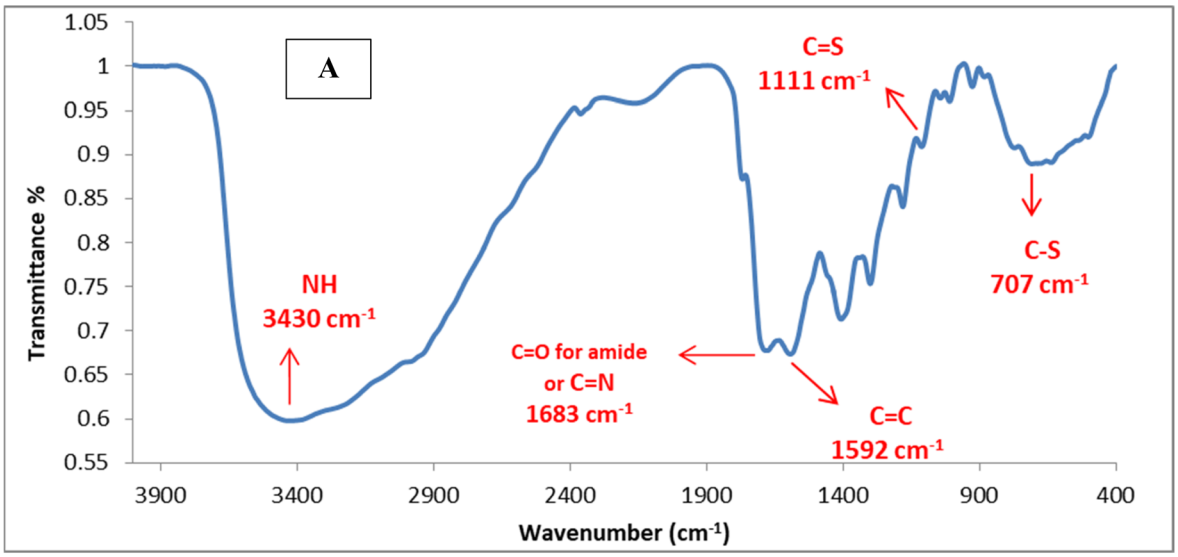

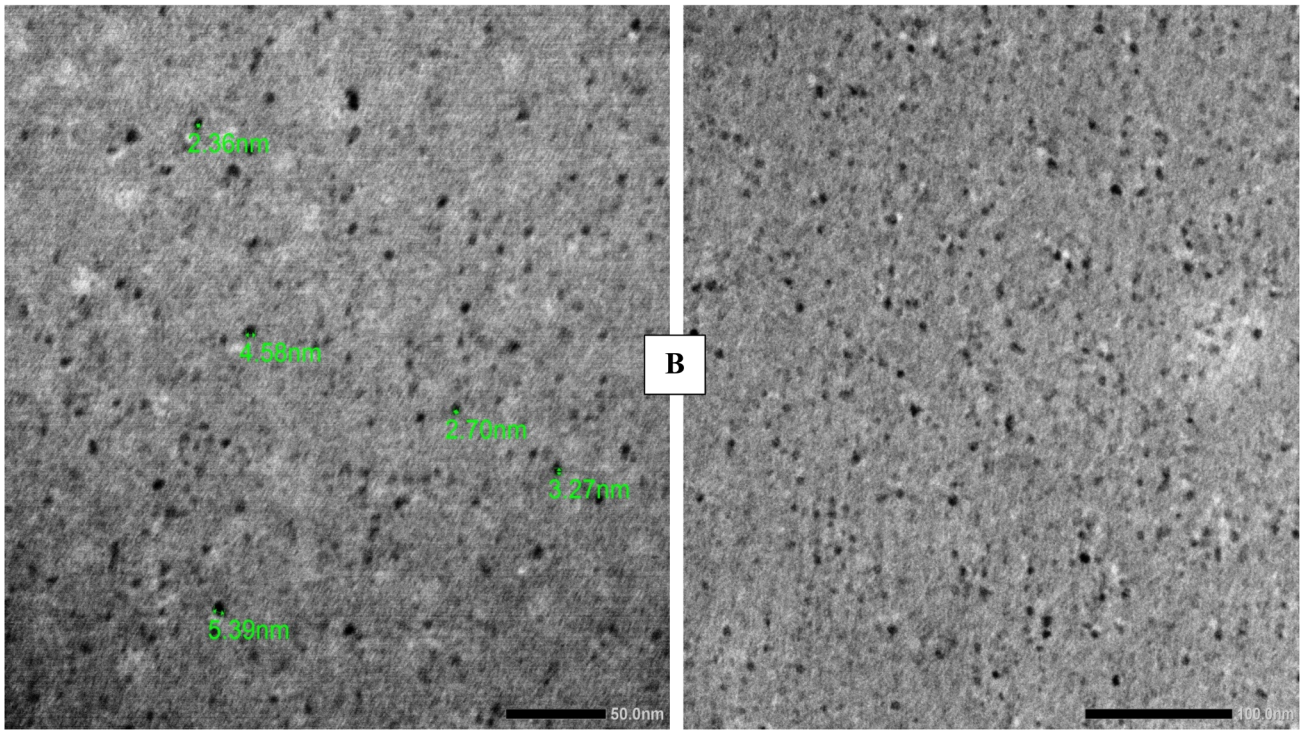

Fig. 2 (A) FTIR spectrum of the N,S-CQDs. (B) TEM images of N,S-CQDs.

steps.[34,35] IFE was formerly considered an anomaly in fluorescence measurements. This effect arises due to the reabsorption of the excitation or emission radiation of the fluorophore by the quencher, leading to a decrease in the luminescence intensities.[36]

This study revealed a significant overlap between the excitation spectrum of the synthesized fluorophore and the drug's absorption spectrum (Fig. 3A and B). Consequently, IFE served as a quenching mechanism.[33] Further mechanisms beyond IFE can occur; the Stern–Volmer equation was employed to identify further mechanisms that may account for the quenching of the fluorophore's luminescence.[37,38]

$$F_0/F = 1 + K_{sv}[\mathrm{FNR}]$$

The luminescence intensities in the absence and presence of the FNR are denoted by F_0 and F, respectively. K_{sv} signifies the Stern–Volmer quenching constant, and [FNR] indicates FNR molar concentration.

In order to distinguish between static and dynamic quenching, the temperature dependency of the Stern–Volmer plot was examined.[35] In dynamic quenching, the Ksv value rises as temperature increases, whereas in static quenching, it drops as temperature increases.[33] At higher temperatures, dynamic quenching happens because diffusion is more efficient,

 © 2025 The Author(s). Published by the Royal Society of Chemistry

Open Access Article. Published on 24 November 2025. Downloaded on 1/19/2026 3:43:59 PM.
This article is licensed under a Creative Commons Attribution-NonCommercial 3.0 Unported Licence.

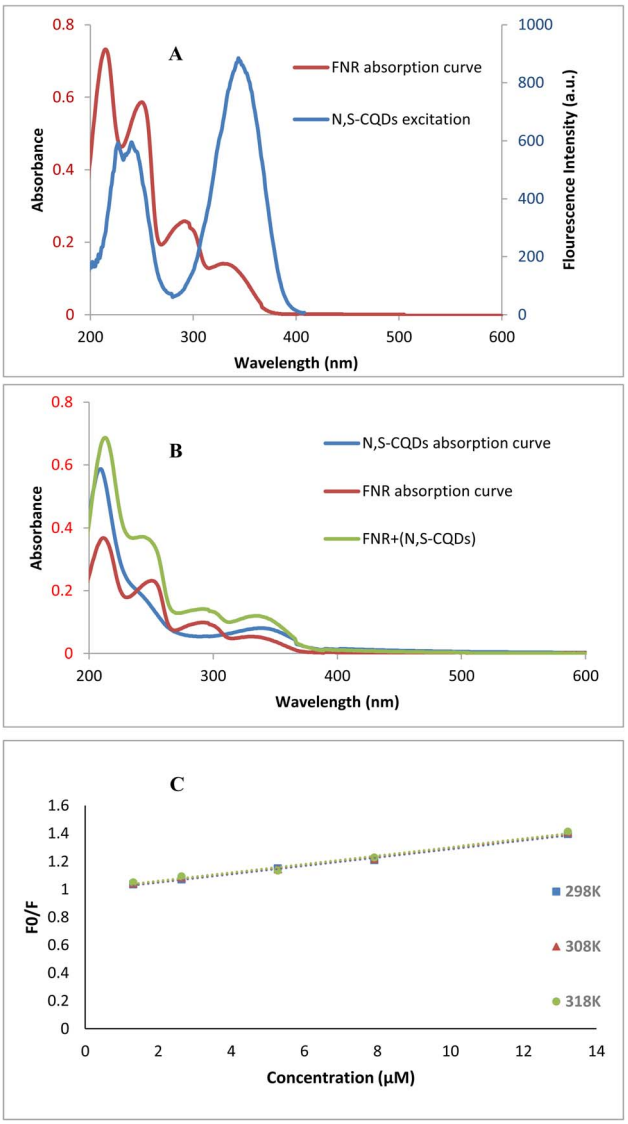

Fig. 3 (A) Absorption spectrum of 6 μg per mL FNR overlayed on the excitation spectrum of N,S-CQDs (λ excitation = 344 nm, λ emission = 419 nm, with excitation/emission slit widths of 5 nm). (B) Absorption spectra of N,S-CQDs, 3 μg per mL FNR, and FNR-(N,S-CQDs) mixture. (C) Stern–Volmer plot of the interaction of different concentrations of FNR with N,S-CQDs at different temperatures (298 K, 308 K, 318 K).

whereas static quenching is typically less effective because weakly bound complexes dissociate at higher temperatures.[35] To achieve this objective, five distinct FNR concentrations were assessed at different temperatures (298 K, 308 K, 318 K), and the resultant Stern–Volmer plots were analyzed (Fig. 3C). The outcomes, illustrated in Fig. 3C, indicate that the K_{sv} constant derived from all plots was approximately 3×10^4 L mol^{-1} and remained unaffected by changing the temperature. Consequently, both dynamic and static quenching are eliminated, confirming IFE as the anticipated quenching mechanism.[16] In order to provide additional verification of the explained mechanisms, UV absorption spectra were plotted for FNR, N,S-CQDs, and FNR-(N,S-CQDs) mixture (Fig. 3B). The absence of any new absorption peaks confirms the absence of a static quenching mechanism.[37,39] The schematic diagram summarizing the sensing mechanism is shown in Fig. S2.

3.4. Reaction parameters optimization

The reaction settings were examined to achieve optimal quenching for the studied medication (3 μg mL^{-1}). Multiple variables were refined. The factors examined included the buffer pH, buffer volume, influence of the diluent solvent, and the reaction duration.

3.4.1. Impact of buffer pH and volume. 0.04 M BR-buffer was utilized to examine the pH impact on luminescence quenching. The impact of various pH levels of the BR-buffer (pH 3, 5, 7, 8, and 9) was examined, revealing the highest quenching impact of the FNR on N,S-CQDs at pH 8.0, as shown in Fig. S3(A). The effect of using different volumes of BR-buffer at pH 8 (ranging from 2 to 8 mL in 2 mL increments) on the quenching power of FNR was examined. The results illustrated in Fig. S3(B) indicate that 2 mL of BR-buffer yielded the most significant quenching effect of FNR. Consequently, 2 mL of BR-buffer (pH 8.0) was selected as the best solution for quenching of the fluorophore with the investigated medication.

3.4.2 Impact of the solvent type. To determine the solvent that elicited the greatest fluorescence quenching of FNR, a diverse array of solvents was implemented as diluted solvents. Deionized water, ethanol, acetonitrile, methanol, and isopropanol were the solvents that were investigated. The fluorescence quenching of FNR using deionized water was found to be the highest based on the results obtained, as illustrated in Fig. S3(C). This can be ascribed to the tendency of more polar solvents, like deionized water, to diminish the energy of π–π^* transition while amplifying the energy of n–π^* transition, hence enhancing the luminescence intensity of the fluorophore.[40] Consequently, deionized water was utilized as the diluent for the method, simplifying the process, reducing costs, and most importantly, enhancing its environmental sustainability.

3.4.3 Impact of reaction time. The inhibitory impact of FNR on the luminescence intensities of the fluorophore was studied throughout time. The FNR–(N,S-CQDs) solution was permitted to stay for 30 minutes at ambient temperature, with the fluorescence signal recorded at 5-minute intervals. Fig. S3(D) illustrates that after adding FNR to the N,S-CQDs, a quick reaction developed at zero time, and the reaction exhibited considerable stability for 30 minutes. Consequently, it was determined that prolonged incubation of FNR with N,S-CQDs did not influence the quenching of the fluorophore luminescence, hence accelerating and simplifying the analytical process.

4. Validation criteria of the proposed spectrofluorimetric methodology

The suggested spectrofluorimetric platform was evaluated under optimized conditions utilizing the synthesized N,S-CQDs, according to the recommendations of the International Conference on Harmonisation (ICH).[41]

Open Access Article. Published on 24 November 2025. Downloaded on 1/19/2026 3:43:59 PM.
This article is licensed under a Creative Commons Attribution-NonCommercial 3.0 Unported Licence.

Table 1 Validation data related to the proposed spectrofluorimetric methodology for FNR estimation

Parameters	Value
λ emission (nm)	419
λ excitation (nm)	344
Linearity range (μg ml^{-1})	0.30–9.00
Intercept	13.55
SD of intercept	1.34
Slope	44.97
SD of slope	0.25
Determination coefficient (R^2)	0.9999
LOD (μg ml^{-1})	0.098
LOQ (μg ml^{-1})	0.297
Accuracy[a] (Mean ± %RSD)	99.82 ± 1.14
Repeatability[b] (%RSD)	0.72
Intermediate precision[b] (%RSD)	1.15

[a] n = mean of five determinations. [b] n = mean of three determinations.

4.1 Linearity, range, LOD, and LOQ

The developed spectrofluorimetric platform demonstrates linearity within the concentration range of 0.30–9.00 μg mL^{-1} under optimized circumstances (Table 1). Fig. 4A illustrates the luminescence emission spectra of the fluorophore following the addition of increasing amounts of FNR, whereas Fig. 4B illustrates the corresponding FNR calibration curve. The curve represents a linear relationship between the difference in luminescence intensities of the fluorophore before (F^0) and after incorporation of FNR (F) against the related FNR concentrations (μg mL^{-1}). The derived regression equation is outlined as $F^0 - F = 44.969C + 13.546$.

At the highest FNR concentration studied (9.00 μg mL^{-1}), the emission intensity decreased significantly from its initial value, resulting in a calculated fluorescence fold decrease of approximately $F_0/F \approx 2$, indicating almost twofold quenching under optimal conditions. Following that, the Limits of Detection and Quantification (LOD and LOQ) for estimating FNR were computed using the formulae defined by the ICH,[41] where LOD = 3.3(S/b) and LOQ = 10(S/b); here, (S) indicates the response standard deviation, while b represents the slope of the calibration curve. LOD and LOQ for FNR were determined to be 0.098 μg mL^{-1} and 0.297 μg mL^{-1}, respectively, demonstrating the high sensitivity of the developed platform (Table 1).

4.2 Accuracy and precision

The accuracy of the suggested spectrofluorimetric platform was assessed by analyzing five different FNR concentrations (0.3, 3.0, 5.0, 7.0, and 9.0 μg mL^{-1}) utilizing the suggested procedure. The obtained % recoveries were satisfactory, confirming the high accuracy of the developed methodology (Table 1). The accuracy of the suggested methodology was also evaluated by the standard addition process for determining the FNR in the commercial formulation and human plasma. Accepted % recoveries were attained (Tables 2 and 3).

The repeatability and intermediate precision of the suggested approach were assessed using 3 different FNR concentrations (1.0, 5.0, and 9.0 μg mL^{-1}) on a single day and over three successive days. Table 1 illustrates the efficacy of the suggested method for FNR estimation, as the RSD% remained under 2%, confirming the remarkable precision of the suggested method.

4.3 Robustness

To assess robustness, the effects of minor fluctuations in experimental settings were evaluated, such as the N,S-CQDs volume (10 ± 1 μL), and the excitation wavelength (344 ± 3 nm), the obtained RSD% values (below 2%) demonstrate that these differences did not substantially influence the analysis of

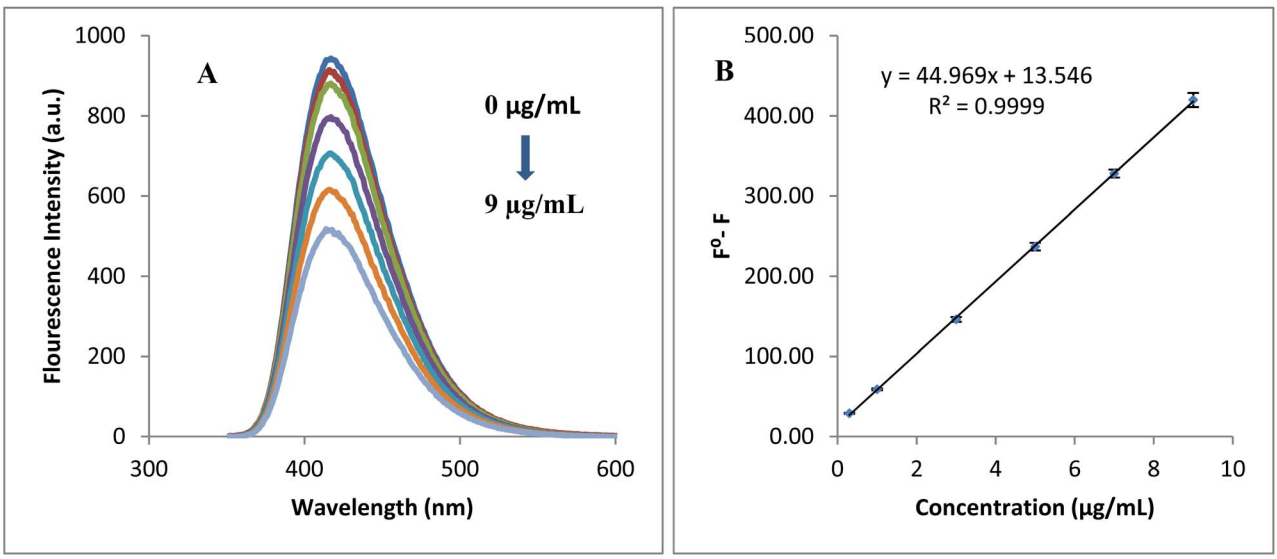

Fig. 4 (A) Fluorescence emission spectra of N,S-CQDs in aqueous solution upon addition of different FNR concentrations (0.0–9.0 μg mL^{-1}), and (B) the corresponding calibration curve.

 © 2025 The Author(s). Published by the Royal Society of Chemistry

Open Access Article. Published on 24 November 2025. Downloaded on 1/19/2026 3:43:59 PM.
This article is licensed under a Creative Commons Attribution-NonCommercial 3.0 Unported Licence.

Table 2 Quantification of FNR utilizing the developed spectrofluorimetric method in pharmaceutical commercial tablets and application of the standard addition technique

Tablets	% Found ± %RSD[a]	Standard addition technique		
		Added (μg mL^{-1})	Founded (μg mL^{-1})	% Recovery[a]
Finoxlab® (20 mg per tab)	99.76 ± 0.57	0.30	0.299	99.67
		1.00	1.008	100.80
		3.00	2.973	99.09
		5.00	4.960	99.19
		7.00	6.947	99.24
		Mean ± %RSD		99.60 ± 0.71

[a] Mean of five determinations.

Table 3 Application of the developed spectrofluorimetric methodology for FNR quantification in spiked plasma samples

Added conc. (μg mL^{-1})	Found conc. (μg mL^{-1})	(%) Recovery[a]	% RSD
0.30	0.301	100.44	1.34
0.40	0.403	100.67	1.58
0.50	0.495	99.07	1.28

[a] Mean of three determinations.

FNR, hence affirming the Robustness of the suggested methodology.

4.4 Selectivity and specificity

The selectivity of the suggested spectrofluorimetric approach for FNR analysis was examined using various interferents that may exist as additives, excipients, or other similar substances found in the human plasma. We investigated the impacts of diverse substances, such as uric acid, ascorbic acid, citric acid, mannitol, starch, glucose, fructose, sucrose, and talc, along with various ions such as Ca^{2+}, Cl^{-}, Mg^{2+}, Na^{+}, and K^{+}, at a concentration of 100 μM. The experimentation revealed that these compounds did not influence N,S-CQDs luminescence. Moreover, these substances did not influence FNR's capacity to suppress N,S-CQDs luminescence (Fig. S4). This phenomenon is elucidated by the lack of these substances from IFE in the emission or excitation spectra of the fluorophore, with the % RSD not surpassing 2%. Moreover, the favorable recovery percentages shown in Tables 2 and 3 indicate that the ingredients co-formulated within the commercial preparations and the naturally occurring substances in human plasma did not influence the suggested luminescence approach. The results illustrated the proposed method's efficacy and specificity for quantifying FNR in diverse matrices.

4.5. Application

4.5.1. Estimation of FNR in commercial pharmaceutical formulation. The FNR concentration in Finoxlab® tablets (20 mg FNR for each tablet) was evaluated to assess the practicality of the proposed methodology. Table 2 shows that the determination of FNR in the commercial tablets was successfully carried out using the suggested methodology, as indicated by the accepted percentage recovery (99.76% with a % RSD of 0.57). The developed method accurately estimates FNR without alteration by any additives found in the commercial product. Moreover, the Student's *t*-test and the variance ratio *F* test were applied to compare the statistical results of the established approach with the spectrofluorimetric reference method.[9] The findings shown in Table 4 revealed no statistically significant disparity between the methodologies.

4.5.2. Estimation of FNR in spiked human plasma. The proposed technique was successfully applied to determine FNR in human plasma accurately. Table 3 shows the results, encompassing the % recoveries of the defined FNR content in the plasma (99.07–100.67%), and the %RSD values did not exceed 2%. The results verified the successful application of the suggested methodology and demonstrated its usefulness for FNR estimation in human plasma without interference. The suggested method demonstrated no significant impact from compounds found naturally in human plasma.

4.6. Evaluation of the ecological sustainability of the suggested spectrofluorimetric methodology

The greenness and ecological friendliness of the suggested spectrofluorimetric platform were investigated using three strategies, namely the Complex Modified Green Analytical Procedure Index (ComplexMoGAPI), the Blue applicability grade index (BAGI), and the Carbon footprint reduction index (CaFRI).

Table 4 Statistical comparison between the proposed and reference methods for FNR analysis

Parameters	Proposed method	Reference method[9]
Mean[a]	99.76	99.92
SD	0.57	0.76
Variance	0.32	0.57
n	5	5
Student's *t*-test	0.37 (2.31)[b]	—
F-test	1.77 (6.39)[b]	—

[a] Mean of five determinations. [b] Parenthesis contain the corresponding theoretical values of *t*-test and *F*-test at 95% confidence limit.

Open Access Article. Published on 24 November 2025. Downloaded on 1/19/2026 3:43:59 PM.
This article is licensed under a Creative Commons Attribution-NonCommercial 3.0 Unported Licence.

4.6.1. ComplexMoGAPI. This is a novel greenness appraisal approach developed to assess the sustainability and greenness of the methods of analysis.[24] It is a modified version of the commonly used programs called complexGAPI[42] and GAPI.[43] The ComplexGAPI does not possess a thorough grading system for analytical approaches, which would facilitate more straightforward comparisons of operations with this tool. Whereas ComplexMoGAPI, on the other hand, is an advanced program that seamlessly combines the aesthetic qualities of ComplexGAPI with precise cumulative grades. The index functions as a widely employed evaluation of the ecological viability of methods of analysis. The assessment is depicted through five pentagrams that provide a comprehensive evaluation of the entire process, including energy usage, waste generation, instrumentation, solvent and reagent utilization, and sample collection and preparation. The pre-analysis techniques are depicted in the hexagonal design at the foundation of the framework. The assessment employs a color system, with red indicating significant detrimental ecological effects, and yellow and green denoting moderate and minimal impacts, respectively. The highest score is 100 (the greenest), and the greenness decreased as the score decreased. Ultimately, the proposed spectrofluorimetric methodology was investigated using this tool, and it exhibited considerable sustainability, evidenced by 15 green zones with a total score of 84 (Fig. 5A).

4.6.2. BAGI. BAGI is an innovative and simple appraisal tool used to assess the adaptability and practicality of every method of analysis. BAGI serves as an adjunct tool to existing greenness assessment methods, highlighting the blue aspects of white analytical chemistry, primarily relevant to practical steps. This method requires the evaluation of ten attributes, encompassing aspects of the analytical technique, such as its kind, necessary instruments/solvents, and degree of automation. Additionally, other sample-related parameters are assessed, including sample volume, the number of simultaneously processed samples/tested analytes, the type of sample preparation, and the testing throughput per hour.[25] The BAGI program is an open-source software that produces a colored pictogram consisting of ten parts, containing a grade at its center. Each section is assigned a consecutive shade of blue/score, with white (2.5), pale blue (5), blue (7.5), and navy blue (10) indicating no, low, medium, or high adherence to the relevant criteria, respectively. The comprehensive final grade spans from 25, denoting the least effective strategy in terms of application, to 100, which signifies the optimal technique efficacy. A minimum threshold of 60 points is required for

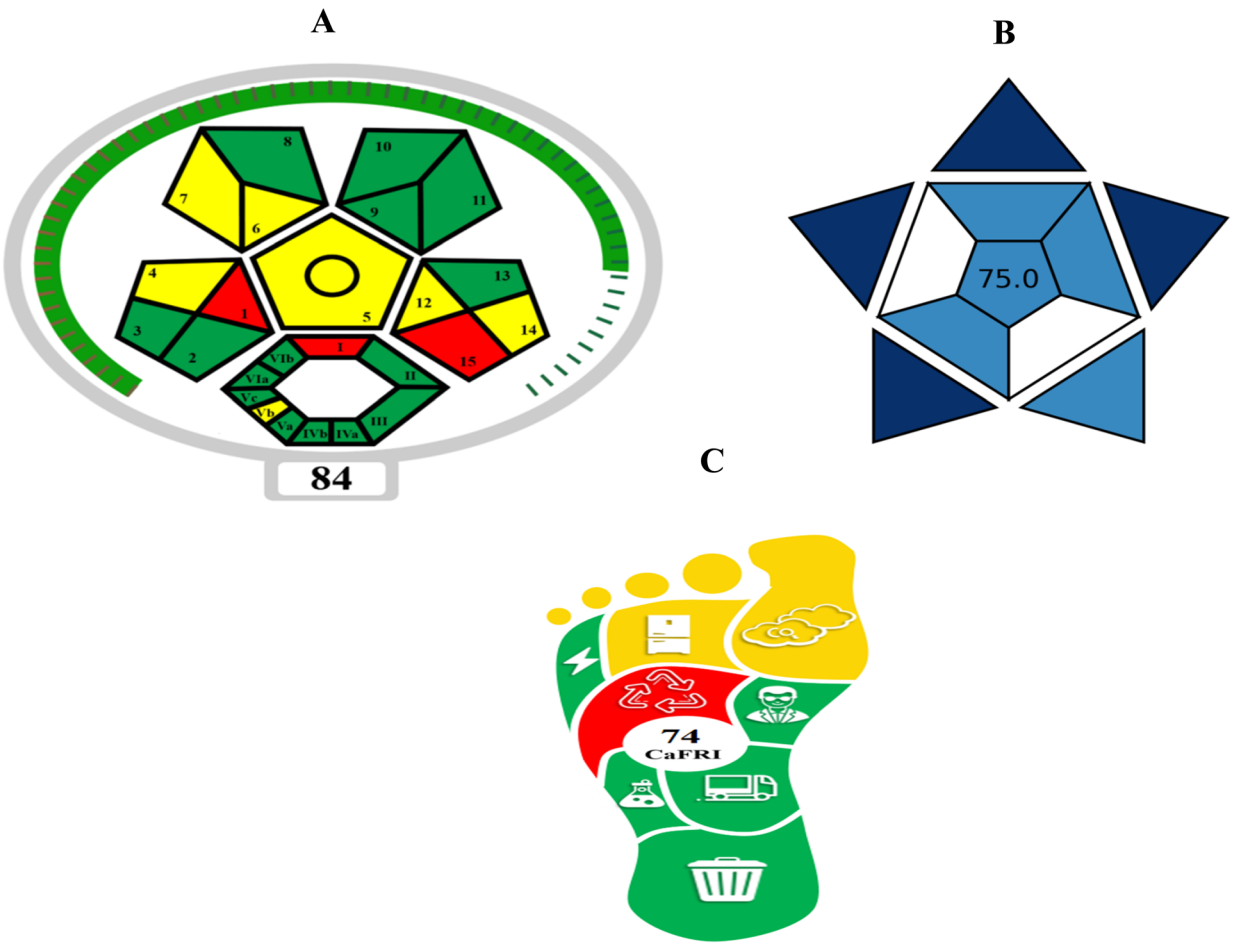

Fig. 5 Method greenness assessment tools: (A) ComplexMoGAPI tool, (B) BAGI tool, and (C) CaFRI tool.

 © 2025 The Author(s). Published by the Royal Society of Chemistry

Open Access Article. Published on 24 November 2025. Downloaded on 1/19/2026 3:43:59 PM.
This article is licensed under a Creative Commons Attribution-NonCommercial 3.0 Unported Licence.

Table 5 Ecological sustainability comparison between the proposed spectrofluorimetric method and other reported methods for FNR estimation

Method	ComplexMoGAPI	BAGI	References
The approach used consecutive reactions to convert FNR into a fluorescent product. The combination of finerenone with trimethylamine forms a nucleophilic intermediate that combines with bromoacetyl bromide to create a fluorescent product	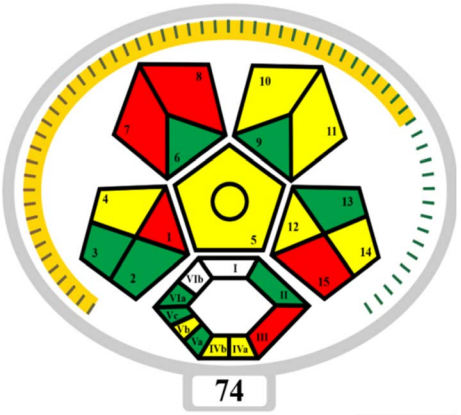		Alsharif *et al.*[9]
A high-performance liquid chromatography–tandem mass spectrometry (HPLC–MS/MS) assay. The autosampler temperature was set at 10 °C. A 80/20 v/v mixture of acetonitrile and ammonium acetate (adjusted to pH 3.0 with formic acid) was used			Rohde *et al.*[10]
FNR quantitative analysis by quenching the fluorescence of N,S-CQDs using deionized water as a diluting solvent			Proposed method

a procedure to be considered "practical". The suggested spectrofluorimetric methodology attained a cumulative score of 75, as it gets high scores in several aspects, such as quantification analysis, simple instrumentation, simple and low-cost preparation procedures, ability to analyze more than ten samples per hour, common commercially available reagents, no preconcentration required, and the need for a small amount of sample, thereby proving its practicality (Fig. 5B).

4.6.3. CaFRI. The CaFRI tool was recently developed to encourage research institutions to consider energy-conserving practices and utilize energy-efficient instruments.[44] This project may stimulate efforts to reduce the carbon impact and strive for greater sustainability. The primary criteria employed

Open Access Article. Published on 24 November 2025. Downloaded on 1/19/2026 3:43:59 PM.
This article is licensed under a Creative Commons Attribution-NonCommercial 3.0 Unported Licence.

for CaFRI assessment include energy usage and CO_2 emissions. Reducing energy consumption, especially by utilizing renewable energy and energy-efficient devices, is crucial for mitigating environmental impacts. Similarly, reducing CO_2 emissions by employing devices with reduced emission parameters and quantifying the carbon footprint is crucial. Furthermore, the CaFRI encourages a single individual to perform the entire procedure, and the waste generated can be disposed of by the same analyst. Other elements that positively affect the overall CaFRI score include transportation and storage, which do not require particular circumstances. These parameters assist the analytical procedure and identify areas requiring further improvement to develop more environmentally friendly techniques. The entirely sustainable procedures for carbon footprint estimation achieve a score of 100. The suggested spectrofluorimetric platform exhibits substantial success in minimizing the carbon footprint, evidenced by a score of 74 (Fig. 5C and Table S1).

4.7. Comparison of the proposed spectrofluorimetric methodology with reported approaches in the literature for FNR analysis

The analytical performance of the suggested methodology was compared with previously published FNR analytical approaches (Table S2), indicating that the suggested approach exhibits high sensitivity and a low detection limit. Although Alsharif *et al.*[9] and Rohde *et al.*[10] reported FNR spectrofluorimetric and HPLC–MS/MS analytical methods, respectively, with higher sensitivity, the suggested methodology is more eco-friendly. The proposed method utilized green reagent (N,S-CQDs), instead of using toxic and negatively ecological impact reagents such as bromoacetyl bromide[45] and trimethylamine,[46] which are used in the reported fluorimetric method.[9] The suggested technique has greater benefits than the documented HPLC–MS/MS method, including cost-effectiveness, simplicity, and the absence of the need for costly instrumentation or complex analytical reagents and toxic solvents. Furthermore, utilizing water as the diluent renders the proposed method a more environmentally friendly alternative to previously documented techniques. Two distinct ecological sustainability assessment tools, namely ComplexMoGAPI and BAGI, were employed to compare the developed methodology with those previously described methods (Table 5). ComplexMoGAPI scores were 74, 77, and 84 for Alsharif *et al.*,[9] Rohde *et al.*,[10] and the proposed methods, respectively. Whereas, BAGI scores were 60, 70, and 75, respectively. These results indicate the superiority of the suggested method in terms of greenness and eco-friendliness.

Conclusion

A sensitive, eco-friendly, and inexpensive fluorescent sensor was constructed for the quantification of FNR. This methodology relied on quenching of the luminescence intensity of N,S-CQDs by FNR *via* the inner filter effect. The preparation procedures for water-soluble N,S-CQDs are straightforward, cost-effective, and provide a high yield. It is dependent on the hydrothermal reaction between glutathione and citric acid. In contrast to the analytical assays for FNR that were previously reported in the literature, this fluorescence sensing system provides a diverse array of advantages. Firstly, the absence of expensive apparatus simplified the operation of this procedure and minimized the associated expenses. Secondly, the computed LOD and LOQ values of this spectrofluorimetric technique were in the nanoscale range, indicating adequate sensitivity. Thirdly, the developed methodology enabled the estimation of FNR in pharmaceutical tablets and human plasma without interference, thereby demonstrating the approach's acceptable reliability and selectivity. Fourthly, this customized approach utilized water as a diluent while employing minimal quantities of organic solvents. Consequently, this study surpasses previous reported FNR analytical methods due to its superior environmental sustainability, which is a critical analytical feature that is currently being extensively studied to guarantee a green analytical approach. Fifthly, this study employed the blue applicability grade index, complex modified green analytical procedure index, and carbon footprint reduction index as methods for assessing the sustainability of the proposed approach, and the accepted scores were obtained reflecting the eco-friendliness of the proposed spectrofluorimetric platform. To sum up, this methodology is characterized by its speed, simplicity, and non-destructive nature, as it does not include laborious pre-treatment processes, derivatization reactions, or toxic reagents, unlike previously reported approaches.

Conflicts of interest

All authors affirm the absence of any conflicts of interest pertaining to the publishing of this research.

Data availability

The authors confirm that the data supporting the findings of this study are available within the article and its supplementary information (SI). Supplementary information is available. See DOI: https://doi.org/10.1039/d5ra07857a.

Acknowledgements

This investigation was not financially supported by any specific entity.

References

1 Pubchem, 2020, https://pubchem.ncbi.nlm.nih.gov/compound/Finerenone, last accessed May 2025.
2 A. K. Singh, A. Singh, R. Singh and A. Misra, *Diabetes Metab. Syndr.*, 2022, **16**, 102638.
3 L. A. Marcath, *Clin. Diabetes*, 2021, **39**, 331–332.
4 Drugbank, 2020, https://go.drugbank.com/drugs/DB16165, last accessed Sebtember 2025.
5 FDA, *Approval of Finerenone*, 2021, https://www.fda.gov/drugs/news-events-human-drugs/fda-approves-drug-reduce-

 © 2025 The Author(s). Published by the Royal Society of Chemistry

Open Access Article. Published on 24 November 2025. Downloaded on 1/19/2026 3:43:59 PM.
This article is licensed under a Creative Commons Attribution-NonCommercial 3.0 Unported Licence.

risk-serious-kidney-and-heart-complications-adults-chronic-kidney-disease, last accessed Sebtember 2025.
6 EMA, https://www.ema.europa.eu/en/medicines/human/EPAR/kerendia, last accessed May 2025, 2022.
7 F. Husnain, P. Mahboob and M. Khaleel, *Asian J. Res. Chem.*, 2023, 16.
8 B. Rajnandani, P. J. Vyas, S. Rathwa, B. Malete, C. N. Shah and U. Upadhyay, *Int. Res. J. Pharmaceut. Sci.*, 2024, **2**, 584–594.
9 S. T. Alsharif, S. l. Alaqel, A. H. Almalki, M. A. Algarni, R. M. Alnemari, M. H. Abduljabbar and A. H. Abdelazim, *Spectrochim. Acta Mol. Biomol. Spectrosc.*, 2024, **309**, 123836.
10 G. Rohde, S. Loewen and R. Heinig, *J. Chromatogr. B*, 2021, **1172**, 122643.
11 Y. V. Reddy, A. Nayak, G. Sangeetha, M. Deepa and R. Kumta, *Biochem. Cell. Arch.*, 2024, **24**, 2331.
12 A. Murugesan and M. Mukthinuthalapati, *Acta Pharm. Sci.*, 2021, **5**, 25–31.
13 G. Magdy, H. Elmansi, F. Belal and A. K. El-Deen, *Curr. Pharm. Des.*, 2023, **29**, 415–444.
14 S. Ross, R.-S. Wu, S.-C. Wei, G. M. Ross and H.-T. Chang, *J. Food Drug Anal.*, 2020, **28**, 677.
15 M. M. Elnaggar, A. F. El-Yazbi, T. S. Belal and H. M. Elbardisy, *RSC Adv.*, 2023, **13**, 29830–29846.
16 N. A. Qandeel, A. A. El-Masry, M. Eid, M. A. Moustafa and R. El-Shaheny, *Anal. Chim. Acta*, 2023, **1237**, 340592.
17 Q. Wang, H. Zheng, Y. Long, L. Zhang, M. Gao and W. Bai, *Carbon*, 2011, **49**, 3134–3140.
18 Y. Dong, C. Chen, X. Zheng, L. Gao, Z. Cui, H. Yang, C. Guo, Y. Chi and C. M. Li, *J. Mater. Chem.*, 2012, **22**, 8764–8766.
19 Y.-P. Sun, B. Zhou, Y. Lin, W. Wang, K. A. S. Fernando, P. Pathak, M. J. Meziani, B. A. Harruff, X. Wang, H. Wang, P. G. Luo, H. Yang, M. E. Kose, B. Chen, L. M. Veca and S.-Y. Xie, *J. Am. Chem. Soc.*, 2006, **128**, 7756–7757.
20 Y. Li, Y. Hu, Y. Zhao, G. Shi, L. Deng, Y. Hou and L. Qu, *Adv. Mater.*, 2011, **23**, 776–780.
21 L. Zheng, Y. Chi, Y. Dong, J. Lin and B. Wang, *J. Am. Chem. Soc.*, 2009, **131**, 4564–4565.
22 M. J. Krysmann, A. Kelarakis, P. Dallas and E. P. Giannelis, *J. Am. Chem. Soc.*, 2012, **134**, 747–750.
23 R. Liu, D. Wu, S. Liu, K. Koynov, W. Knoll and Q. Li, *Angew. Chem., Int. Ed.*, 2009, **48**, 4598–4601.
24 F. R. Mansour, K. M. Omer and J. Płotka-Wasylka, *Green Anal. Chem.*, 2024, **10**, 100126.
25 N. Manousi, W. Wojnowski, J. Płotka-Wasylka and V. Samanidou, *Green Chem.*, 2023, **25**, 7598–7604.
26 F. R. Mansour and P. M. Nowak, *BMC Chem.*, 2025, **19**, 121.
27 Y. Ganjkhanlou, J. J. E. Maris, J. Koek, R. Riemersma, B. M. Weckhuysen and F. Meirer, *J. Phys. Chem. C.*, 2022, **126**, 2720–2727.
28 A. R. Nallayagari, E. Sgreccia, L. Pasquini, F. Vacandio, S. Kaciulis, M. L. Di Vona and P. Knauth, *Electrochim. Acta*, 2022, **427**, 140861.
29 X. Zhao, H. Wang, Q. Liu and X. Chen, *Talanta*, 2024, **269**, 125479.
30 O. A. Aladesuyi and O. S. Oluwafemi, *Inorg. Chem. Commun.*, 2023, **153**, 110843.
31 X. Zhai, P. Zhang, C. Liu, T. Bai, W. Li, L. Dai and W. Liu, *Chem. Commun.*, 2012, **48**, 7955–7957.
32 S. M. Mohyeldin, W. Talaat, M. F. Kamal, H. G. Daabees, M. M. T. El-Tahawy and R. M. Keshk, *Sci. Rep.*, 2024, **14**, 2927.
33 G. Magdy, S. Ebrahim, F. Belal, R. A. El-Domany and A. M. Abdel-Megied, *Sci. Rep.*, 2023, **13**, 5502.
34 Y. Song, S. Zhu, S. Xiang, X. Zhao, J. Zhang, H. Zhang, Y. Fu and B. Yang, *Nanoscale*, 2014, **6**, 4676–4682.
35 W. Talaat, A. A. Farahat and R. M. Keshk, *Biosensors*, 2022, **12**, 1005.
36 H. M. Elbardisy, T. S. Belal, M. M. T. El-Tahawy, W. Talaat and R. M. Keshk, *Luminescence*, 2025, **40**, e70077.
37 M. A. Alossaimi, H. Elmansi, M. Alajaji, A. Altharawi, A. S. A. Altamimi and G. Magdy, *Molecules*, 2023, **28**, 2351.
38 M. S. Nasr, M. M. Y. Kaddah, S. Morshedy, G. Omran and W. Talaat, *Heliyon*, 2024, **10**, e32120.
39 G. Magdy, F. Belal and H. Elmansi, *RSC Adv.*, 2023, **13**, 4156–4167.
40 R. S. Haggag, D. A. Gawad, S. F. Belal and H. M. Elbardisy, *Anal. Methods*, 2016, **8**, 2479–2493.
41 P. Ravisankar, C. N. Navya, D. Pravallika and D. N. Sri, *IOSR J. Pharm.*, 2015, **5**, 7–19.
42 J. Płotka-Wasylka and W. Wojnowski, *Green Chem.*, 2021, **23**, 8657–8665.
43 J. Płotka-Wasylka, *Talanta*, 2018, **181**, 204–209.
44 F. Mansour and P. Nowak, *BMC Chem.*, 2025, **19**, 121.
45 PubChem, *Bromoacetyl bromide*, 2004, https://pubchem.ncbi.nlm.nih.gov/compound/Bromoacetyl-bromide, last accessed September 26, 2025.
46 ACS, *Trimethylamine*, 2022, https://www.acs.org/molecule-of-the-week/archive/t/trimethylamine.html, last accessed September 26, 2025.